We are IntechOpen, the world's leading publisher of Open Access books
Built by scientists, for scientists

6,900
Open access books available

186,000
International authors and editors

200M
Downloads

Our authors are among the

154
Countries delivered to

TOP 1%
most cited scientists

12.2%
Contributors from top 500 universities

CLARIVATE ANALYTICS
BOOK CITATION INDEX
INDEXED

WEB OF SCIENCE™

Selection of our books indexed in the Book Citation Index
in Web of Science™ Core Collection (BKCI)

Interested in publishing with us?
Contact book.department@intechopen.com

Numbers displayed above are based on latest data collected.
For more information visit www.intechopen.com

Pan-sharpening Methods based on ARSIS Concept

Mehran Yazdi and Arash Golibagh Mahyari
School of Electrical and Computer Engineering, Shiraz University,
Iran

1. Introduction

Pan-sharpening aims to use image fusion techniques in the remote sensing field in order to synthesis the Multispectral (MS) images to higher resolution using spatial information of the Panchromatic (Pan) image. Up to now, several definitions for the image fusion have been suggested. Wald's definition (Wald, 1999) is one of these most celebrated definitions used commonly in the remote sensing community which defines image fusion as: "a formal framework in which are expressed means and tools for the alliance of data originating from different sources. It aims at obtaining information of a greater quality, although the exact definition of 'greater quality' will depend on the application". Many applications such as feature detection, change monitoring, urban analysis, and land cover classification recieve benefits of pan-sharpening. In fact, these applications need both high spectral and spatial resolution concurrently. Due to physical and technological constraints, creating a sensor which can provide high spectral and spatial resolution simultanously is not possible. So, the image fusion algorithms have been received increasingly attention to fuse MS and Pan images and to provide a new image including both spatial charachteristics of Pan and spectral charachteristics of MS images. Usually the pan-sharpening methods are categorized into three main sets (Wald, 2002; Thomas et al., 2008);projection substitution, relative spectral contribution, and methods that belong to the Amélioration de la Résolution Spatiale par Injection de Structures (ARSIS) concept.

The Projection–Substitution methods take advantage of a vectorial algorithm. In this kind of methods, all fused images corresponding to different MS images are synthesized simultaneously. These methods consider coincident pixels of MS images as spectral axes. Then, the spectral axes are projected into a new space to reduce the information redundancy. It results the decorrelated components. The structures of MS images, which are mainly related to color, are isolated by one of these components from the rest of the information. Actually these methods assume that the structures contained in this structural component are equivalent to those in the Pan image. Next, this structural component is replaced either partially or wholly with corresponding parts of Pan. Eventually, the inverse projection is performed to obtain the MS images in higher resolution, i.e. the fused images. The most famous methods of this category are those based on principal component analysis (PCA) (Ehlers, 1991; Chavez et al., 1991) and intensity hue saturation (IHS) (Haydn et al., 1982).

The Relative Spectral Contribution methods are also based on the linear combination of bands. The basic assumption of these methods is considering the low-resolution Pan as a

linear combination of original MS images. This assumption arises from the overlap of the spectral bands. Besides, a filtering operation applied on the Pan image is implicitly required. In addition, the fused MS product is a function of this linear combination and of the Pan image as well. Brovey (Gillespie et al, 1987) is the most important algorithm of this category. The high correlation between the Pan and each MS images is the most important factor of the two mentioned categories which affects the fusion results. The higher the correlation between the Pan and each MS images is, the better the outcome of fusion will be. If the correlation of Pan and MS image is large, the MS image can be considered as an affine function of the Pan image. Moreover, the most characteristic of these two types of methods is their spectacular increase in visual impression with a good geometrical quality. So, they are well adapted to certain applications such as cartography or the localization of specific phenomena like target recognition (Vijayaraj et al, 2004; Yocky, 1996).Nevertheless, their major disadvantage is spectral distortion, called the color or radiometric distortion, characterized by inclining to present a predominance of a color on the others. However, their spectral distortion arises from the modification of the low frequencies of the original MS images (Shi et al, 2005). It means while no obvious relation exists between Pan and MS input modalities, creating the fused image as a function of the original MS and Pan images leads to this spectral distortion. Another disadvantage of these two types is that they apply the same model to the entire image (Thomas et al., 2008).

The third category is ARSIS concept which is the French acronym for "Amélioration de la Résolution Spatiale par Injection de Structures" meaning Improving Spatial Resolution by Structure Injection. The fundamental assumption of this type is that the missed spatial information in MS image can be derived from the high frequencies laying between orignial and low spatial version of the Pan, and possibly from external knowledge. This type is what would be discuused more in the following.

However, some other methods, called Hybrid methods, are possible which do not exclusively belong to one of the mentioned categories. They may include more than one category (Thomas et al., 2008). One of these renowned categories is projection–substitution combined with relative spectral contribution. Those methods which combine IHS method with spectral contribution assumption are the examples of this hybrid category. The relative spectral contribution combined with the ARSIS concept assumption is another famous category of hybrid methods. They are based on the minimization of energy functional. The third celebrated hybrid category is the projection–substitution combined with the ARSIS concept assumption. Many recent methods such as improved IHS method (González-Audícana et al, 2004), improved adaptive PCA method (Shah et al, 2008), etc can be put in this category.

In the following, more focuces will be placed on the ARSIS concept and it would be reviewed in more details. Then, some renowned methods based on ARSIS concept will be discussed. Finally, the simulation results of the described methods would be presented.

2. ARSIS concept

As mentioned in previous section, in ARSIS concept, synthesizing the MS image in higher resolution is seen as the inference of the information missing in the original MS image. The fundamental assumption of ARSIS concept is that the missing information is linked to the high frequencies of Pan and MS images. Indeed, finding this relationship between high frequencies in Pan and MS images is the thing that investigated in the ARSIS concept.

Methods based on ARSIS concept usually perform the following steps: at first, the required information should be elicited from Pan image; next, the missing information in MS image must be inferred using the extracted information; finally, the MS image in high resolution would be synthesized (Ranchin & Wald, 2000; Ranchin et al, 2003).

Although diverse algorithms for ARSIS concept are possible, the majority of recent algorithms apply multiscale or multiresolution transforms on both Pan and MS images to obtain a scale by scale description of the images content information. This description, called multiscale model (MSM), is usually represented by a pyramidal structure as shown in Figure 1 (Thomas et al., 2008).
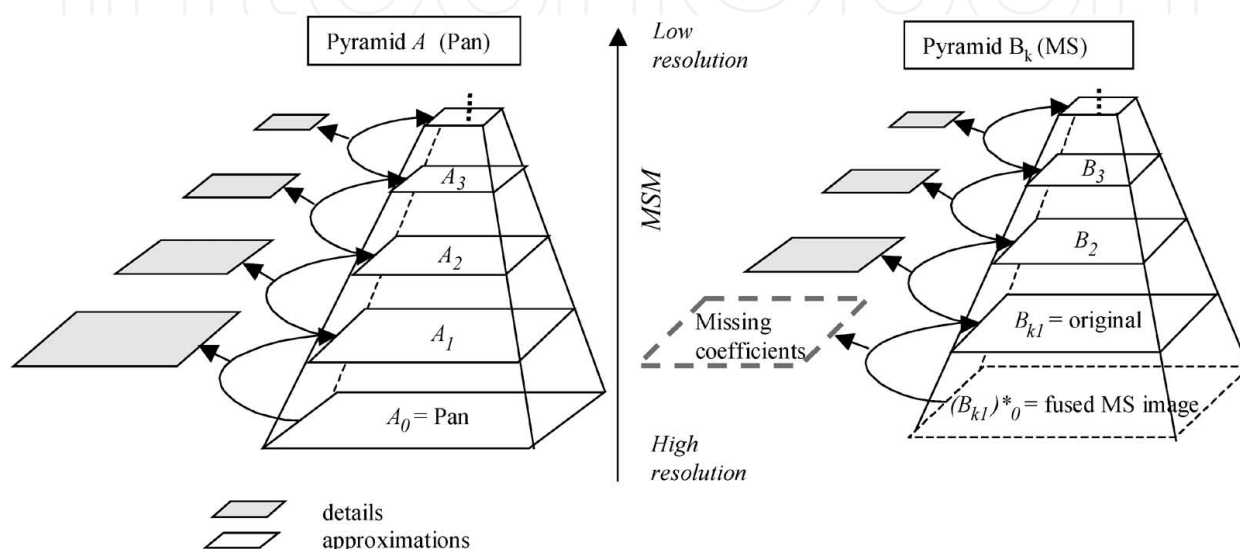

Fig. 1. Pyramidal structure of information (Thomas et al., 2008)

In this structure, the missing high frequency information of MS image, shown by dashed line in pyramid B, is extracted from the corresponding details in Pan image, which is displayed by gray parallelogram in pyramid A, to synthesize the MS image in higher resolution as indicated by dashed line in the bottom of pyramid B. However, if the extracted information from Pan is inserted directly into the missing high frequency information of MS image, the synthesized MS image may not be the same as "what would be seen if the MS image were taken by an especial sensor at Pan's resolution". Consequently, some adaption or transformation, called the intermodality model (IMM) (Wald, 2002) or the interband structure model (IBSM) (Ranchin et al, 2003), should be applied to adjust the extracted information to MS image. Figure 2 shows the ARSIS fusion procedure. Up to now, several IMM have been proposed (Ranchin et al, 2003; Aiazzi et al, 2002).

On the other hand, there are many methods like High Pass Filtering (HPF) method (Chavez et al., 1991) in which the extracted information are injected without any transformation into the low-resolution MS image. However, MSM might employ different transforms like Laplacian Pyramid (LP), Wavelet (Mallat, 1999), Curvelet (Starck et al, 2002), etc, to decompose and synthesize Pan and MS.

However, as the consistency property indicates (Thomas & Wald, 2004), if a fused product is downsampled to its original resolution, the original MS image must be restored. Since MSMs utilize mutiresolution algorithms to decompose input images into low and high frequency parts, they can isolate low frequencies from high frequencies and preserve the low frequencies while synthesizing high frequencies. Furthermore, in many papers it is
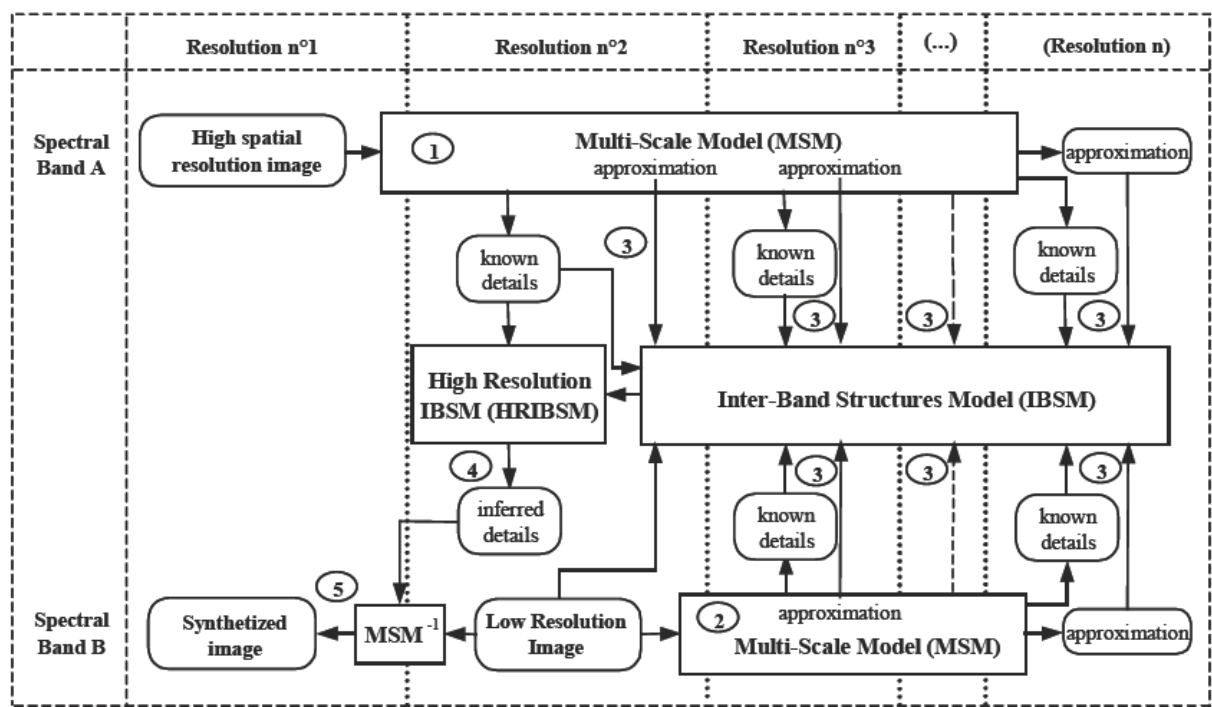
Fig. 2. General scheme for the application of the ARSIS concept (Ranchin et al, 2003)

mentioned that the multiresolution algorithms can provide a good trade off between preserving the low frequencies and injecting the high frequencies (Wald, 2002; Thomas et al., 2008; Ranchin et al, 2003). Nevertheless, multiscale algorithms should be selected in such a way that they do not produce artifacts affecting low frequencies like aliasing.

Likewise, many fusion methods are based on local estimation of parameters to take into account local dissimilarities between Pan and MS images. In these methods, the injection will be performed in such way that the local parameters meet certain demands. Although these methods assure good consistency with the original MS image, several experiments have demonstrated that it might decline the quality of the results and weakens image interpretation (Thomas et al., 2008).

However, the ARSIS concept is still being noticed by many researchers. We will discuss some of the famous ARSIS-based methods in more details in the following. Our discussion would concentrate on AABP model (Aiazzi et al, 2001), context driven method (Aiazzi et al, 2002) and the fusion method based on Linear Test Dependency (Golibagh Mahyar & Yazdi, 2010; 2009).

3. AABP model

The AABP (the model of Aiazzi, Alparone, Baronti and Pippi) proposed by Aiazzi *et al.* belongs to IBSM models (Aiazzi et al, 2001). As it was mentioned, IBSM models deal with the transformation of spatial structures with changes in spectral bands. Their model takes into account the relationship between the details or context of Pan and MS images.

In this method, the input images are decomposed into approximation and details coefficients by a multiresolution transform such as LP or wavelet. Let D_{MS}^l and D_{Pan}^l be the detail coefficients of MS and Pan images at certain resolution l, respectively. In addition, let C_{MS}^l and C_{Pan}^l be the approximation coefficients of input images. The AABP model tries to

discover a local relationship between D_{MS}^l and D_{Pan}^l. This relationship is calculated by considering C_{MS}^l and C_{Pan}^l. In this model, it is assumed that the detail coefficients of MS can obtain by scaling the detail coefficients of Pan. This relation is defined as:

$$D_{MS}^l = \alpha \,.\, D_{Pan}^l \tag{1}$$

Where α is a coefficient representing the local relationship. Considering Figure 1, the missing coefficients in pyramid B are calculated by Eq. (1). In order to synthesize the MS image at a higher resolution, first Pan should be decomposed into a lower resolution. The obtained detail coefficients of Pan at this resolution are used to estimate the missing coefficients of the MS image in Eq. (1). Then, in order to acquire the proper value of α, the approximation coefficients of Pan and MS image are decomposed into a lower resolution. After calculating α, the missing coefficients of MS image can easily be anticipated by multiplying α at detail coefficients of Pan at the first level of decomposition. Finally, the synthesized MS image at a higher resolution can be created simply by computing the inverse multiresolution transform using original MS image as the approximation coefficients and estimated missing coefficients as the detail coefficients. This procedure is shown in Figure 3.
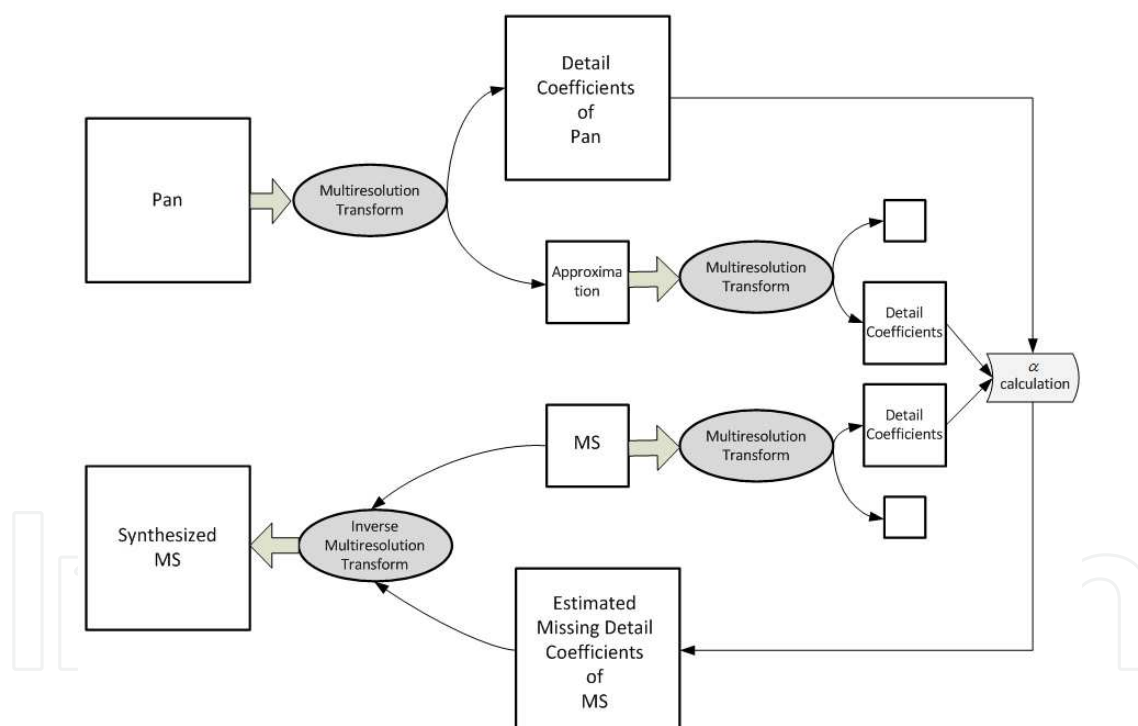

Fig. 3. Flowchart of AABP model

Furthermore, the calculation of α is performed in a $n \times n$ sliding window around each coefficient, typically 9×9 for IKONOS images. Let σ_{Pan} and σ_{MS} be the standard deviation of Pan's and MS's detail coefficient in this window. In addition, consider ρ as the local correlation coefficient between Pan's and MS's detail coefficient. Let also θ be a constant threshold. This threshold can have any value in the interval $[0.3 , 0.6]$; however the higher value of threshold is usually selected in condition that the correlation coefficient is not very large. According to these assumptions, α is chosen based on the below rule.

$$\alpha = \begin{cases} \min\left(\dfrac{\sigma_{MS}}{(1+\sigma_{Pan})} , 3 \right) & if \ \rho \geq \theta \\ 0 & if \ \rho < \theta \end{cases} \qquad (2)$$

To avoid numerical instabilities on homogenous areas of Pan, α is clipped above 3 in the first row of Eq. (2).

4. Context driven method

Similar to many methods in which the high frequencies of Pan are modified before injecting into MS, Context-driven method employs statistical measures in order to locally give weights to the high frequency coefficients of Pan. Moreover, this method uses a statistical criterion to make decision whether or not the high frequency coefficients obtained from Pan should be injected into the high frequency coefficients of MS. This decision rule is based on comparing the statistical criterion, which measures in turn the matching degree between the low-pass version of Pan and the expanded MS, using a specific threshold. Although the context-driven method can be implemented by any multiresolution transform, here we explain the algorithm based on wavelet transform.

In order to register the input images, original MS image should be upsampled by two and then passed into an 23-taps pyramid-generating lowpass filter. Next, Pan and upsampled MS are decomposed by wavelet transform. Let D_{MS}^{k} ; $k=H,V,D$ and D_{Pan}^{k} ; $k=H,V,D$ be the detail coefficients of MS and Pan images respectively where $k=H,V,D$ stand for Horizontal, Vertical and Diagonal coefficients. In addition, let C_{MS} and C_{Pan} be the approximation coefficients of input images. Firstly, the local correlation coefficient is calculated for every approximation coefficient. So, around $(i,j)th$ approximation coefficient in MS and Pan decomposed images, an $n \times n$-window is considered to compute the local correlation coefficient, named $LCC(i,j)$, between Pan and MS approximations; later during fusion process, $LCC(i,j)$ will be compared with the certain threshold θ. Furthermore, in order to create weighted Pan's detail coefficients before injecting into MS's detail coefficients, a local weight is calculated for $(i,j)th$ approximation coefficient; this weight is defined as the ratio of the standard deviation of MS image, which is locally computed in the $n \times n$ window among approximation coefficients of MS, to the standard deviation of Pan, locally computed in the $n \times n$ window among approximation coefficients of Pan. This weight for the $(i,j)th$ coefficient is $\gamma(i,j)$. Now, the $(i,j)th$ detail coefficient in all three subbands $k=H,V,D$ are injected, according to the rule in Eq. (3), into the corresponding location in MS's detail coefficient only if the $LCC(i,j)$ is greater than θ. The latter constraint is to avoid entering the unlikely unrelated details.

$$D_{MS}^{k} = \begin{cases} \gamma . D_{Pan}^{k} & if \ LCC \geq \theta \\ D_{MS}^{k} & Otherwise \end{cases} \ ; \ k=H,V,D \qquad (3)$$

Figure 4 shows the fusion procedure of this algorithm diagrammatically.
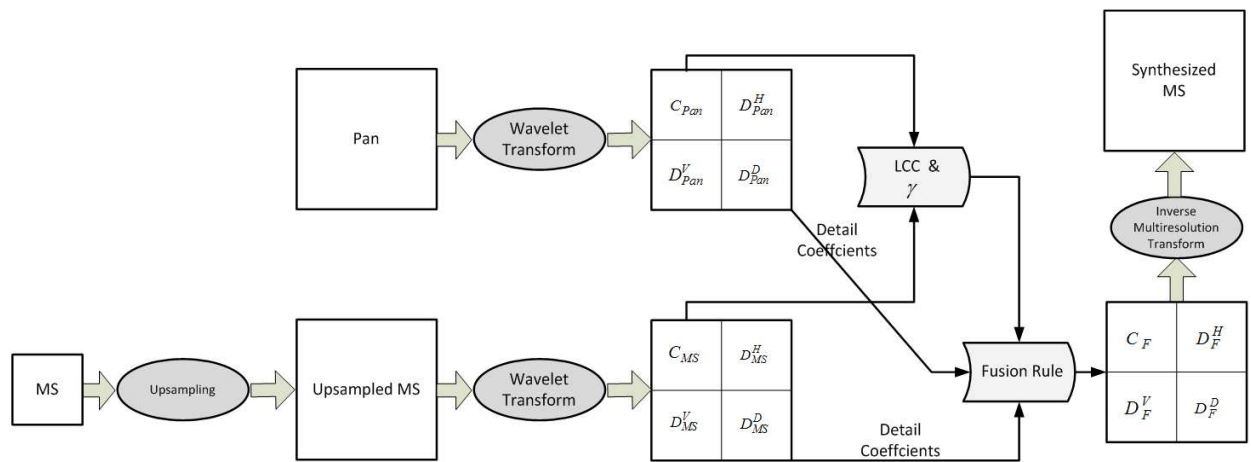
Fig. 4. Flowchart of fusion process based on context-driven method

5. GLP-SDM

Like other methods, the main goal of this method is to preserve the spectral information of MS images during the injection of high frequency details by means of selectively substituting the spatial-frequencies spectrum of Pan into MS image. In fact, the main idea of this method is based on minimizing the spectral distortion during fusion process which is performed by serving the Spectral Angle Mapper (SAM) as a criterion. However, the missing details are injected into the upsampled MS image after scaling them.

Suppose that h is the scaling ratio (e.g. $h = 2$ for Landsat images) between Pan and original MS images, namely the size of Pan is h times greater than that of original MS. Let MS be the original MS image, Pan be the Pan image and F be the fused image or enhanced MS image. In order to synthesize the MS image at higher resolution, first the original MS image is upsampled by h to create the upsampled MS image $\tilde{MS}$. Then $\tilde{MS}$ is passed into the h-expansion lowpass filter e_h whose cutoff frequency is equal to $\frac{1}{h}$ to prevent aliasing. On the other hand, in order to obtain the missing details, a low resolution version of Pan should be created. So, Pan is passed into the h-reduction lowpass filter r_h with cutoff frequency $\frac{1}{h}$ to avoid aliasing and then downsampled the results by h. Afterwards, the downsampled Pan is upsampled by h and passed into the h-expansion lowpass filter e_h with cutoff frequency $\frac{1}{h}$. This leads to the upsampled low resolution Pan image $\tilde{Pan}$. The difference between the upsampled low resolution Pan image and the original one is the missing details which must be injected into the upsampled MS image. Before injecting, the missing details must be rescaled. The proper gain, which can weigh the missing details appropriately, is defined as the ratio of the upsampled MS image ($\tilde{MS}$) over the upsampled low resolution Pan image; it means

$$\gamma = \frac{\tilde{MS}}{\tilde{Pan}} \tag{4}$$

Eventually, the final enhanced MS image is obtained by multiplying γ by the missing details and then adding the result to the upsampled MS image. The mentioned procedure is displayed in Figure 5.
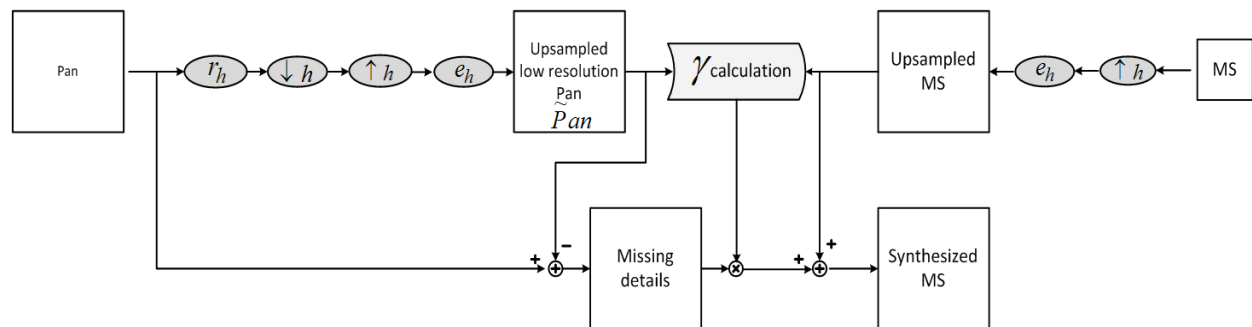
Fig. 5. Blockdiagram of GLP-SDM method

6. Fusion method based on linear dependency test

As it was pointed out, the MSMs use a multiresolution transform to decompose input images in order to efficiently represent their details. The choice of multiscale decomposing algorithm is crucial since it leads to improve the performance of fusion algorithm noticeably. Recently, beyond wavelets such as curvelet, contourlet, etc were proposed. The higher performance of these transforms in well representing details rather than LP and wavelet were proven (Starck et al, 2002). So, this method based on linear dependency test takes the advantages of curvelet transform (Starck et al, 2002). In addition, an appropriate fusion rule can increase the performance of fusion method significantly. Selecting the detail coefficients with the maximum absolute value is one of the simple fusion rules. However, fusion decision based on coefficient values alone can inject noise into the final image. As a result, not only the fusion algorithm won't enhance the spatial resolution of MS image, but also it will decline the spatial and spectral resolution of original MS image. So, in this method the detail coefficients are opted regionally. The outlandish details like lines are distributed among neighbouring detail coefficients. Therefore, in order to determine whether there is an outlandish feature in the vicinity of a detail coefficient, the linear dependency test is used in this method which is computed in a window centred on a certain coefficient detail. In the following, the basic concept of curvelet transform will be explained and then the fusion method based on the linear dependency test will be presented.

6.1 Discrete curvelet transform

Curvelets can be seen as an extension of wavelets for multidimensional data. The key difference between the wavelet and curvelet is that only curvelets are really directional. Curvelets satisfy the anisotropic scaling relation $width \approx length^2$ in the spatial domain (Candes & Donoho, 2000). For example, as shown in Figure 6(a), it would take many wavelet coefficients to accurately represent such a curve. Compared with wavelets, curvelets can represent a smooth contour with much fewer coefficients for the same precision (Figure 6(b)).

Curvelets are defined as a function of $x = (x_1, x_2)$ at scale 2^{-j}, orientations θ_l and positions $x_k^{(j,l)} = R_{\theta_l}^{-1}(k_1.2^{-j}, k_2.2^{-j})$ in the form of:

$$\varphi_{j,k,l}(x) = \varphi_j(R_{\theta_l}(x - x_k^{(j,l)})) \tag{5}$$

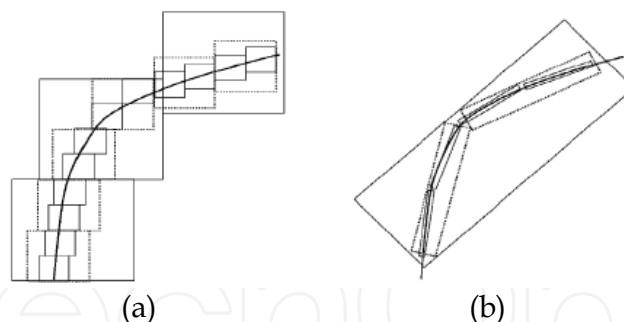(a)   (b)

Fig. 6. Comparison of non-linear approximation performance of wavelet and curvelet. (a) wavelet representation, (b) curvelet representation

where R_θ indicates amount of rotation by θ radians and for rotation angular we have $\theta_l = 2\pi . 2^{-\lfloor j/2 \rfloor} l$; $l = 0,1,2,...$, such that $0 \le \theta_l \le 2\pi$. $\varphi_j(x)$ is a waveform defined in the frequency domain as $\hat{\varphi}_j(\xi) = U(\xi)$ where $U(\xi)$ is defined in the polar coordinates as:

$$U_j(r,\theta) = 2^{-3j/4} W(2^{-j} r) V(\frac{2^{\lfloor j/2 \rfloor} \theta}{2\pi}) \tag{6}$$

where $W(r)$ is the "radial window" supported on $r \in (0.5, 2)$ and $V(t)$ is the "angular window" supported on $t \in [-1,1]$.

A curvelet coefficient is then simply the inner product between an element $f \in L^2(R^2)$ and a curvelet $\varphi_{j,l,k}$,

$$c(j,l,k) = < f, \varphi_{j,l,k} > = \int_{R^2} f(x) \cdot \overline{\varphi}_{j,k,l} dx \tag{7}$$

According to Plancherel's theorem, the above equation can be expressed as the integral over the frequency plane

$$c(j,l,k) = \frac{1}{(2\pi)^2} \int \hat{f}(\xi) \overline{\hat{\varphi}}_{j,l,k}(\xi) d\xi$$
$$= \frac{1}{(2\pi)^2} \int \hat{f}(\xi) U_j(R_{\theta_l} \xi) e^{i < x_k^{(j,l)}, \xi >} d\xi \tag{8}$$

In (Candes et al, 2006), Candes *et al.* proposed two fast discrete curvelet transforms .The first one is a digital transformation which is based on unequally-spaced fast Fourier transforms (USFFT) and another is based on the wrapping of specially selected Fourier samples. We use the first fast discrete curvelet transform to decompose an image into its curvelet coefficients.

6.2 Fusion rule

At the first step, input images, Pan and MS, must be registered. It can be done by interpolating the MS image. Then, the registered images are decomposed by curvelet transform in order to set aside low frequencies for avoiding distortion. The low frequency part of MS image would be considered as the low frequency part of final image.

Furthermore, the linear dependency test is exerted to decide which detail coefficient should be injected into the MS detail coefficients. The linear dependency test can be performed based on either Wronskian determinant (Golibagh Mahyar & Yazdi, 2009) or Gramian (Golibagh Mahyar & Yazdi, 2010). For an $M \times N$ image I, Wronskian's determinant is calculated using Eq. (9)

$$D = \sum_{m=1}^{M} \sum_{n=1}^{N} C^2(m,n) - C(m,n) \qquad (9)$$

In addition, the Gramian is defined as follows (Barth, 1999).

$$G(v_1, v_2, ..., v_N) = \det\left(I^* I\right)$$
$$I = \left(v_1 \; v_2 \; .... \; v_N\right) \qquad (10)$$

Where $C(m,n)$ is the $(m,n)th$ pixel and v_i is an M-dimensional vector of all pixels located in the ith column of the image.

In order to attain $(m,n)th$ detail coefficient of output image, an $W \times W$ window is considered around $(m,n)th$ detail coefficient of MS and Pan images. Then the linear dependency test is computed in this window based on either Eq. (9) or Eq. (10). The higher the value of Wronskian's determinant or Gramian is, the more prominent feature is inside the window. So this value can be compared between MS details and Pan ones to determine which input image has the stronger feature at the $(m,n)th$ detail coefficient. As a consequence, the detail coefficients of Pan will be injected to the final image only if this value in Pan details is greater than the value in MS details. Therefore, it will prevent the injection of noise and non-related details. The fusion rule in this method is defined as:

$$D_F(m,n) = \begin{cases} D_{Pan}(m,n) & if \;\; LD_{Pan}(m,n) \geq LD_{MS}(m,n) \\ D_{MS}(m,n) & if \;\; LD_{Pan}(m,n) < LD_{MS}(m,n) \end{cases} \qquad (11)$$

Where $LD_{MS}(m,n) \; and \; LD_{Pan}(m,n)$ are the value of linear dependency test which can be computed using either Eq. (9) or Eq. (10), respectively. In addition, $D_{Pan}(m,n)$, $D_{MS}(m,n)$, $and \; D_F(m,n)$ are the detail coefficients of Pan, MS and resulted fusion image, respectively. Figure 7 shows the flowchart of this algorithm.

7. Objective indicators

Generally, the quality of fusion process can be investigated either visually or quantitatively. Although a visual assessment gives better view about the quality of image fusion method owing to its dependence on human interpretation, it is not an appropriate way to compare different fusion methods. On the other hand, a quantitative assessment is more suitable to compare methods inasmuch since it is based on numerical values. However, some famous indicators are employed in this chapter in order to compare the mentioned fusion methods with each other. They are as follows.
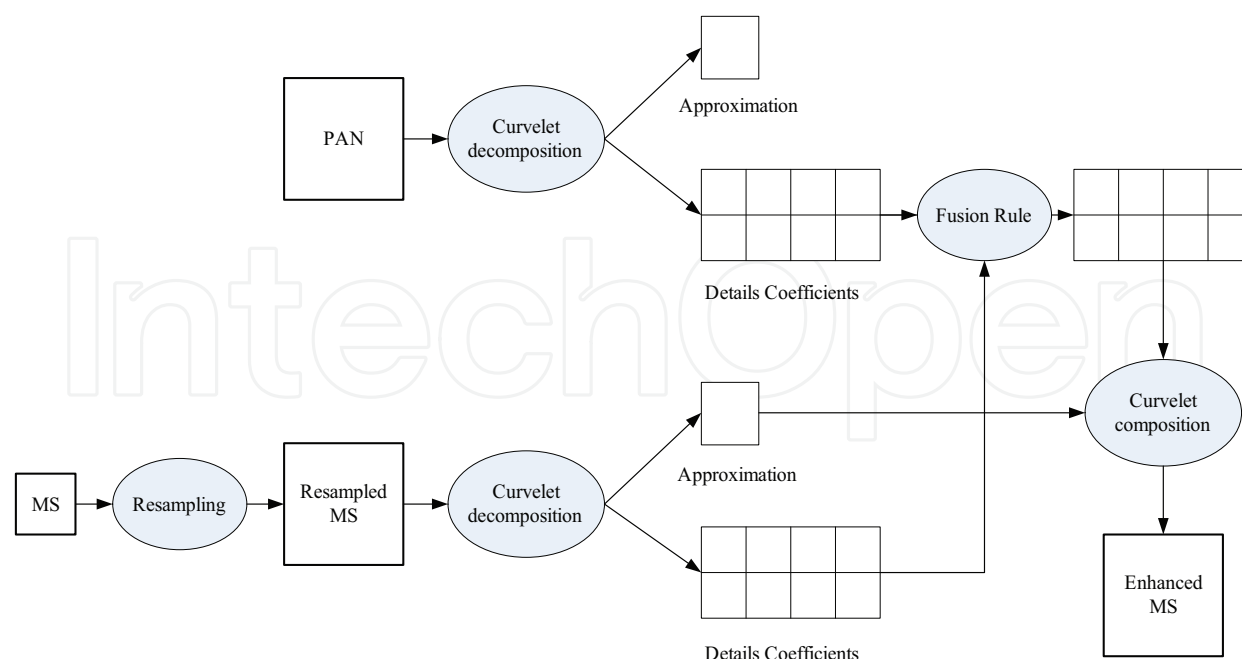
Fig. 7. Flowchart of fusion method based on linear dependency test

7.1 Erreur Relative Globale Adimensionnelle de Synthèse (ERGAS)

It means the relative global dimensional synthesis error and is defined as (Ranchin & Wald, 2000; Ranchin et al, 2003):

$$ERGAS = 100\frac{h}{l}\sqrt{\frac{1}{N}\sum_{i=1}^{N}\frac{RMSE^2(B_i)}{M_i^2}} \qquad (4)$$

where h is the resolution of the high spatial resolution image, l is the resolution of the low spatial resolution image, M_i is the mean radiance of each spectral band involved in the fusion and RMSE is the root mean square error computed by:

$$RMSE^2(B_i) = bias^2(B_i) + SD^2(B_i) \qquad (5)$$

The lower the value of the ERGAS is, the higher the spectral and spatial quality of the fused image will be.

7.2 Spectral Angle Mapper (SAM)

The spectral angle mapper for two given spectral vectors v and $\hat{v}$ is defined as (Ranchin & Wald, 2000; Ranchin et al, 2003):

$$SAM(v,\hat{v}) = \arccos\left(\frac{<v,\hat{v}>}{\|v\|_2\|\hat{v}\|_2}\right) \qquad (6)$$

where $v = \{v_1, v_2, ..., v_L\}$ is the original spectral pixel vector $v_l = \tilde{G}^{(l)}(i,j)$ and $\hat{v} = \{\hat{v}_1, \hat{v}_2, ..., \hat{v}_L\}$ is the distorted vector obtained by applying the fusion process on the coarser resolution of

MS images, i.e. $\hat{v}_l = \hat{G}^{(l)}(i,j)$. SAM is calculated in degree for each pixel and is averaged on all pixels to obtain a single value.

The lower the value of the SAM is, the higher the spectral and spatial quality of the fused image will be.

7.3 Universal Image Quality Index (UIQI)

It is defined as (Wang & Bovik, 2002):

$$Q = \frac{\sigma_{\tilde{G}\hat{G}}}{\sigma_{\tilde{G}}\sigma_{\hat{G}}} \cdot \frac{2m_{\tilde{G}}m_{\hat{G}}}{m_{\tilde{G}}^2 + m_{\hat{G}}^2} \cdot \frac{2\sigma_{\tilde{G}}\sigma_{\hat{G}}}{\sigma_{\tilde{G}}^2 + \sigma_{\hat{G}}^2} \tag{7}$$

The UIQI is designed by modeling any image distortion as a combination of three factors: loss of correlation, radiometric distortion, and contrast distortion.

The greater the value of the UIQI is, the higher the spectral and spatial quality of the fused image will be.

7.4 Correlation Coefficient (CC)

It is defined as (Khan, 2008):

$$CC_{A,B} = \frac{1}{M \times N} \frac{\sum_{i=1}^{M}\sum_{j=1}^{N}(A(i,j) - \mu_A)(B(i,j) - \mu_B)}{\sqrt{\left(\sum_{i=1}^{M}\sum_{j=1}^{N}(A(i,j) - \mu_A)^2\right)\left(\sum_{i=1}^{M}\sum_{j=1}^{N}(B(i,j) - \mu_B)^2\right)}} \tag{8}$$

It is calculated between fused image and reference image.

8. Experimental results and discussion

A sample data set, which was obtained from LandSat ETM+, is used in order to evaluate the described methods. This satellite provides seven multispectral images in bands 1-7 and one panchromatic image in band 8. These bands are in three different resolution categories as follows.

- 30 m for bands 1–5 and 7;
- 60 m for band 6;
- 15 m for band 8.

According to the spectral range of these 8 bands, only three bands 2, 3 and 4 have overlap with spectral range of Pan which is why only these three bands are used to fuse with Pan and assess the fusion methods' performance. These three bands can be displayed as an RGB image.

The outcomes of applying AABP, context-driven, GLP-SDM and Fusion Method based on Linear Dependency Test methods are depicted in Figure 8.

In order to compare different methods, the original MS image in Figure 8(b) is set as the reference. AABP method (whose fusion result is shown in Figure 8(c)) not only did not enhance the resolution of the upsampled MS image (Figure 8(a)) but also injected noise and led the fusion result to become blurred. In addition, this method caused spectral distortion
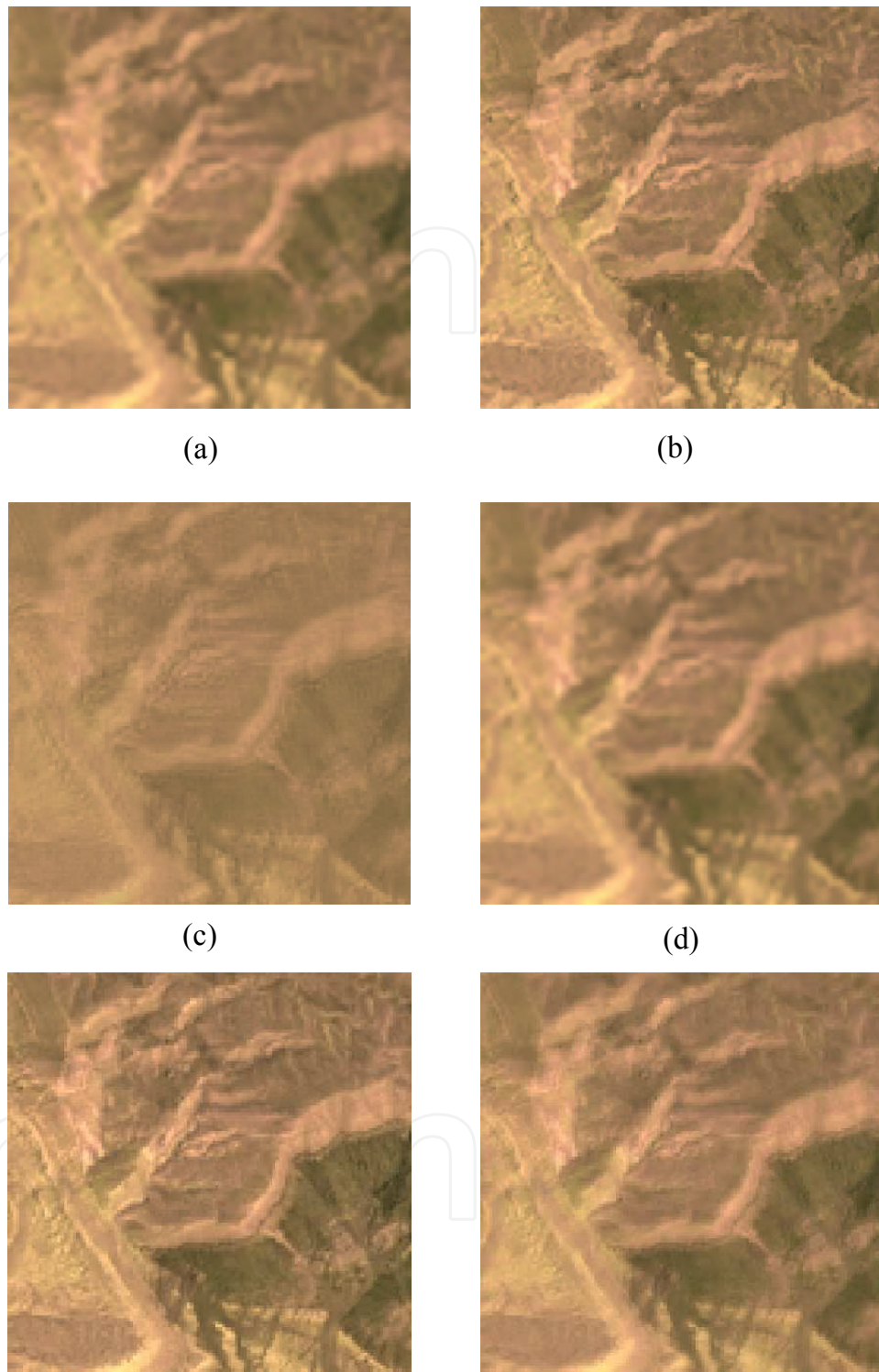
Fig. 8. Experimental results obtained using different methods; (a) upsampled low resolution MS; (b) original MS; Fusion results of (c) AABP model; (d) context-driven; (e) GLP-SDM; (f) Linear dependency test

in the final result which can be seen especially in the left-down corner of the image where mustered color was turned to bright brown. On the other hand, the context-driven method in the Figure 8(d) preserved the spectral content of MS image; it also enhanced the spatial resolution somehow but the image was still blurred. Unlike these two methods, the fusion results of GLP-SDM method was enhanced noticeably. Furthermore, visually comparison does not indicate any spectral distortion. Finally, the method based on linear dependency test provided enhancements in upsampled MS image. Moreover, no spectral distortion can be identified in the fusion outcome.

However, evaluation criteria can provide a better comparison among various methods. So that these four methods are compared numerically in Table 1 using described evaluation criteria in the previous section.

	ERGAS	SAM	UIQI	CC
AABP Model	3.73	1	0.29	0.73
Context-Driven	1.49	0.72	0.85	0.92
GLP-SDM	1.57	0.65	0.88	0.95
Linear Dependency Test	1.39	0.71	0.89	0.96

Table 1. Evaluation Criteria comparison

Sure enough, the AABP model has the worst performance among these four methods according to Table 1. On the other hand, although the evaluation criteria values of the other three methods are very close to each other, GLP-SDM and Linear Dependency Test methods have better outcomes in compare with context-driven method. Likewise, the performance of Linear Dependency Test method in spatial enhancement is little better than that of GLP-SDM method. Nevertheless, according to SAM, the GLP-SDM method preserves the spectral content better as it is clear from a visual comparison.

9. Conclusion

In this chapter, the ARSIS concept, one of the most important categories for the image fusion, was considered. The basic assumption of ARSIS concept is the existence of a relationship between high frequency components of Pan and MS images. So, the majority of fusion methods in this category incline to decompose input images by a multiresolution transform in order to separate high frequencies from low frequencies resulting in preservation of low frequencies during the fusion process.

Furthermore, four novel fusion methods were elaborated. Eventually, the methods were compared visually and assessed quantitatively based on some well-known criteria. However, further works on ARSIS concept would be appreciated by introducing newer multiresolution transform like ridgelet, surfacelet, etc.

10. References

Aiazzi, B.; Alparone, L.; Baronti, S.; & Pippi, I. (November 8-9th 2001). Quality assessment of decision-driven pyramid-based fusion of high resolution multispectral with panchromatic image data. *Proceedings of the IEEE/ISPRS Joint Workshop on Remote Sensing and Data Fusion over Urban Areas*, Rome, Italy, pp. 337-341.

Aiazzi, B.; Alparone, L.; Baronti, S.; & Garzelli, A. (Oct. 2002). Context-Driven Fusion of High Spatial and Spectral Resolution Images Based on Oversampled Multiresolution Analysis. *IEEE Transaction on Geoscience and Remote Sensing*, vol. 40, no. 10, pp. 2300-2312.

Barth, N.R. (1999). The Gramian and K-Volume in N-Space: Some Classical Results in Linear Algebra. *Journal of Young Invest. parallelograms by Frank Jones*.

Candes, E., Donoho, D.L. (2000): Curvelets: a surprisingly effective non-adaptive representation of objects with edges. Vanderbilt University Press, Nashville, TN. ISBN. 0-8265-1357-3.

Candes, E., Demanet, L., Donoho, D.L., Ying, L. (2006): Fast Discrete Curvelet Transform. www.curvelet.org.

Chavez, P. S.; Sides, Jr, S. C. & Anderson, J. A. (1991). Comparison of three different methods to merge multiresolution and multispectral data: Landsat TM and SPOT panchromatic, *Photogrammetric Engineering and Remote Sensing*, vol. 57, no. 3, pp. 295–303.

Ehlers, M. (1991). Multisensor image fusion techniques in remote sensing, *ISPRS Journal of Photogramm and Remote Sensing*, vol. 51, pp. 311–316.

Gillespie, A. R.; Kahle, A. B. & Walker, R. E. (Aug. 1987). Color enhancement of highly correlated images — II Channel ratio and 'chromacity' transformation techniques, *Remote Sensing of Environment*, vol. 22, no. 3, pp. 343–365.

Golibagh Mahyar, A. & Yazdi, M. (7-9March 2009). A Novel Image Fusion Method Using Curvelet Transform Based on Linear Dependency Test, *The 1nd International Conference on Digital Image Processing (ICDIP 2009)*, p.p. 351-354, Thailand.

Golibagh Mahyar, A. & Yazdi, M. (2010). Remote Sensing Image Fusion using Gramian as a Rule of Fusion, *accepted in International Journal of Electronics*.

González-Audícana, M.; Saleta, J. L.; Catalán, R. G. & García, R. (Jun. 2004). Fusion of multispectral and panchromatic images using improved IHS and PCA mergers based on wavelet decomposition, *IEEE Transaction on Geoscience and Remote Sensing*, vol. 42, no. 6, pp. 1291–1299.

Haydn, R.; Dalke, G. W.; Henkel, J. & Bare, J. E. (1982). Application of the IHS color transform to the processing of multisensor data and image enhancement, *Proceeding of International Symposium of Remote Sensing Arid, Semi-Arid Lands*, pp. 599–616, Cairo, Egypt.

Khan, M. M. ; Chanussot, J. ; Condat, L.; & Montanvert, A. (Jan 2008). Indusion: Fusion of Multispectral and Panchromatic Images Using the Induction Scaling Technique, *IEEE Geoscience and Remote Sensing Letters*, vol. 5, no. 1, p.p. 98-102.

Mallat , S. (1999). *A Wavelet Tour of Signal Processing*, Academic Press, 2nd Edition.

Ranchin, T. & Wald, L. (Jan. 2000). Fusion of high spatial and spectral resolution images: The ARSIS concept and its implementation, *Photogrammetric Engineering and Remote Sensing*, vol. 66, no. 1, pp. 49–61.

Ranchin, T.; Aiazzi, B.; Alparone, L.; Baronti, S.; & Wald, L. (Jun. 2003). Image fusion — The ARSIS concept and some successful implementation schemes, *ISPRS Journal of Photogrammetric and Remote Sensing*, vol. 58, no. 1/2, pp. 4–18.

Shah, V. P.; Younan, N. H.; & King, R. L. (May 2008). An Efficient Pan-Sharpening Method via a Combined Adaptive PCA Approach and Contourlets, *IEEE Transactions on Geoscience and Remote Sensing*, vol. 46, no. 5, pp. 1323–1335.

Shi, W.; Zhu, C.; Tian, Y. & Nichol, J. (Mar. 2005). Wavelet-based image fusion and quality assessment, *International Journal of Applied Earth Observation Geoinformation*, vol. 6, no. 3/4, pp. 241–251.

Starck , J.L., Candès, E.J., Donoho, D.L. (Jun. 2002). The Curvelet Transform for Image Denoising. *IEEE Transaction on Image Processing*, vol. 11, no. 6, pp.670-684.

Thomas, C. & Wald, L. (May 25–27, 2004). Assessment of the quality of fused products, *Proceeding of 24th EARSeL Symposium on New Strategies for European Association of Remote Sensing*, Dubrovnik, Croatia, Oluic, Ed. Rotterdam, The Netherlands: Millpress, pp. 317–325.

Thomas, C.; Ranchin, T,; Wald, L. & Chanussot, J. (May 2008). Synthesis of Multispectral Images to High Spatial Resolution: A Critical Review of Fusion Methods Based on Remote Sensing Physics, *IEEE Transaction on Geoscience and Remote Sensing*, vol. 46, no. 5, pp. 1301–1312.

Vijayaraj, V.; O'Hara, C. & Younan, N. (2004). Quality analysis of pansharpened images, *Proceeding of IEEE IGARSS*, vol. 1, pp. 85–88.

Wald, L. (May 1999). Some terms of reference in data fusion. *IEEE Transaction on Geoscience and Remote Sensing*, vol. 37, no. 3, pp. 1190–1193.

Wald, L. (2002). *Data Fusion: Definitions and Architectures. Fusion of Images of Different Spatial Resolutions*. Les Presses de l'école des Mines, ISBN: 978-2-911762-38-3, Paris, France.

Wang, Z.; & Bovik, A.C. (March 2002). A Universal Image Quality Index, *IEEE Signal Processing Letters*, vol. 9, no. 3, pp. 81-84.

Yocky, D. A. (1996). Multiresolution wavelet decomposition image merger of Landsat Thematic Mapper and SPOT panchromatic data, *Photogrammetric Engineering and Remote Sensing*, vol. 62, no. 9, pp. 1067–1074.

Image Fusion

Edited by Osamu Ukimura

Image fusion technology has successfully contributed to various fields such as medical diagnosis and navigation, surveillance systems, remote sensing, digital cameras, military applications, computer vision, etc. Image fusion aims to generate a fused single image which contains more precise reliable visualization of the objects than any source image of them. This book presents various recent advances in research and development in the field of image fusion. It has been created through the diligence and creativity of some of the most accomplished experts in various fields.

How to reference

In order to correctly reference this scholarly work, feel free to copy and paste the following:

Mehran Yazdi and Arash Golibagh Mahyari (2011). Pansharpening Methods Based on ARSIS Concept, Image Fusion, Osamu Ukimura (Ed.), ISBN: 978-953-307-679-9, InTech, Available from: http://www.intechopen.com/books/image-fusion/pansharpening-methods-based-on-arsis-concept